Afdelingen for Bærende Konstruktioner
Department of Structural Engineering
Danmarks Tekniske Universitet • Technical University of Denmark

Triaxial Tests with Concrete and Cement Paste

Thomas Cornelius Hansen

Serie R No 319 1995

Triaxial Tests with Concrete and Cement Paste

Thomas Cornelius Hansen

Triaxial Tests with Concrete and Cement Paste

Tryk:
Afdelingen for Bærende Konstruktioner
Danmarks Tekniske Universitet
Lyngby
ISBN 87-7740-156-5
ISSN 0909-587X
Bogbinder:
H. Meyer, Bygning 101, DTU

Contents

I Preface

This report is the result of a project carried out at the Department of Structural Engineering, Technical University of Denmark, under the supervision of Prof.dr. techn. M.P.Nielsen.

The project is a subproject under a major project financed by the Danish Technical Research Council (STVF).

I would like to thank my supervisor for giving valuable inspiration and encouragement during the project.

The tests presented in the report were performed by M.Sc Claus Schmidt. A sincere thank is given for all his help during the project.

Finally I express my gratitude to all other persons, who contributed to the completion of this report.

Lyngby, December 1994

Thomas Cornelius Hansen

II Abstract

The main purpose of this paper is to present some triaxial tests with concrete and cement paste, and to examine the failure criterion of these materials. The report is subdivided into 5 sections:

1) A short theoretical introduction.
2) Description of the test equipment and the test procedure.
3) Presentation of the test results.
4) Discussion.
5) Conclusion.

The main issue is to examine whether Coulombs failure criterion is sufficient to describe the failure behavior of concrete and paste under triaxial loading. The main conclusion is that the parameters in Coulombs failure criterion are not constants, and that the angle under which failure takes place is varying with the magnitude of the side pressure. Therefore it is necessary to modify the Coulomb failure criterion for concrete and cement paste.

III Resume

Hovedformålet med denne rapport er at præsentere nogle triaxiale forsøg med beton og cementpasta, og at undersøge brudkriteriet for disse materialer. Rapporten er inddelt i 5 afsnit, som indeholder:
1) En kort teoretisk introduktion.
2) Beskrivelse af forsøgsudstyret og forsøgsgangen.
3) Præsentation af forsøgsresultaterne.
4) Diskussion.
5) Konklusion.
Hovedformålet er at undersøge om Coulombs brudkriterium kan benyttes til at beskrive brudopførslen af beton og pasta under triaxial belastning. Hovedkonklusionen er at parametrene i Coulombs brudkriterium ikke er konstante, samt at vinklen under hvilken brud indtræffer varierer med sidetrykkets størrelse. En modifikation af Coulombs brudbetingelse for beton og pasta er derfor nødvendig.

VI Notation

σ	Normal stress
σ_1	Principal stress, side pressure
σ_3	Principal stress, axial pressure
τ	Shear stress
f_c	Compression strength
f_t	Tensile strength
ϵ	Strain
ϵ_1	Lateral strain
ϵ_3	Axial strain
ν	Poissons ratio
v	Failure angle
φ	Angle of friction
c,μ,k	Constants in Coulombs failure criterium

1 Introduction

The main purpose of this paper is to present some triaxial test results with concrete and cement paste. The test series have been carried out to examine the failure criterion of concrete and cement paste.
Several tests have been performed in the past showing that the well-known Coulomb failure criterion (1773) is not valid for large values of normal stress σ, see for instance **[92.2]** and **[93.1]**. The slope of the failure line tends to flatten out in a σ - τ diagram for large σ. In the case of very small values of the normal stress, the slope is larger than the slope defined by the Coulomb failure criterion, see **[93.1 pp.68]**. These phenomena are schematically shown in figure 1.1.

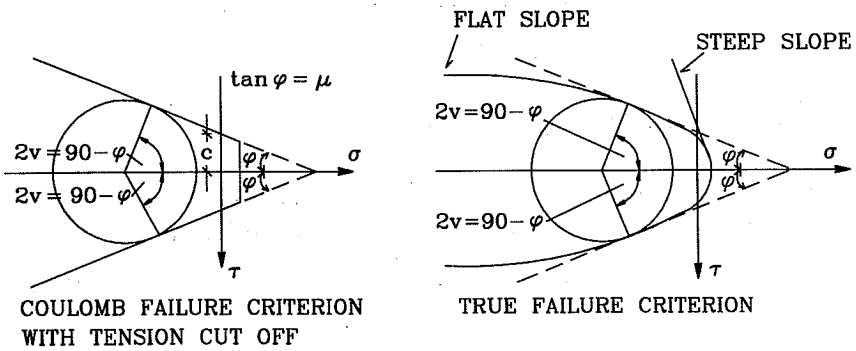

Figure 1.1 *Failure criterion for concrete.*

In this paper particular emphasis is given to examine the behavior for small normal stresses.

Coulombs failure criterion for sliding is (tensile stresses positive):

$$|\tau| = c - \mu\sigma \qquad \textbf{(1.1)}$$

where **c** and **μ** are positive constants, see figure 1.1. The parameter **c** is called the cohesion and **μ** is the coefficient of friction.
In a compression test the friction angle φ is related to the angle **v** of the fracture planes as shown in figure 1.2.

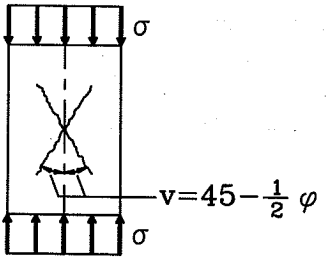

Figure 1.2 *Fracture angle in concrete under compression.*

The failure criterion **(1.1)** can be expressed by the principal stresses σ_1 and σ_3 using Mohr's circle. The result is for $\sigma_1 \geq \sigma_3$, see for instance **[91.1]**:

$$k\sigma_1 - \sigma_3 = 2c\sqrt{k} = f_c \qquad \textbf{(1.2)}$$

where

$$k = (\mu + \sqrt{1+\mu^2})^2 \qquad \textbf{(1.3)}$$

or

$$\mu = \frac{k-1}{2\sqrt{k}} \qquad \textbf{(1.4)}$$

The slope of the fracture planes therefore may be described by the constant k as well as by the constant μ. When k = 1, cf. μ=0 , the slope is flat in a σ - τ diagram, see figure 1.1.

Another useful expression derived in **[91.1 pp.360]** is:

$$\sqrt{k} = \tan(45+\varphi/2) \qquad \textbf{(1.5)}$$

The test results presented will show that the slope of the failure line varies from about k = 8 for small values of σ_1 to almost k = 1 for large values of σ_1. Usually k equal to 4 has been applied for concrete when using the Coulomb failure criterion.
It will further be shown that the angle of the fracture planes approximately follows the relation in formula **(1.5)**.
The value of k can be found by means of a σ_1 - σ_3 diagram. If the theory of perfectly plastic materials with the associated normality condition for strain increments is valid **k** may also be found by determining the slope of the relation ε_1 - ε_3, as illustrated in figure 1.3. We have, see **[91.1]**:

$$k = \frac{\Delta\epsilon_1}{|\Delta\epsilon_3|} \qquad \textbf{(1.6)}$$

If the strain field at fracture is localized as is normally the case in uniaxial conditions or when the side pressure is small, strain measurements on the test specimens as a whole are not representative for what is going on in the fracture planes and it will not be possible to use formula (1.6).

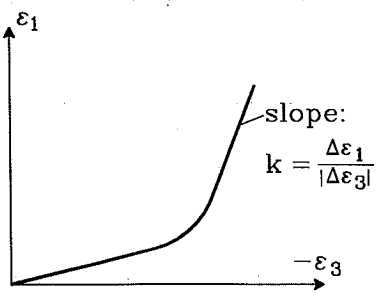

Figure 1.3 *Lateral strain versus axial strain*

2 Test equipment and procedure

In this section the test equipment and procedure will be presented.

Normally in a triaxial compression test a steady side pressure is applied around the cylinder and hereafter the axial pressure is increased until failure. The side pressure is supplied using oil. The axial pressure is supplied by an external jack acting on the specimen by means of a piston. In this case two of the principal stresses are equal, hereafter referred to as the side pressure σ_1, and the third principal stress is the axial pressure σ_3.

In the following a short description of the basic test facilities for the triaxial tests is given. A more detailed description can be found in **[92.1]**.
The triaxial cell is shown in figure 2.1, to which all numbers in the following refers. The cell consists of three major parts: a base unit, a barrel section enclosing the main pressure chamber, and a piston used to apply the axial load from the external jack.

The base unit acts as a base plate (9) for the concrete specimen (8). Furthermore the base unit contains a pipe to fill the cell with oil (16) creating the side pressure.

The barrel section is lowered down over the base plate, and is locked by three clamping sections (11).

The piston moves through two oil chambers, the main chamber (7) and the upper chamber (2). The two chambers are linked, so that equal pressures exist in the two chambers. This ensures that no resultant force is acting on the piston when the oil pressure is raised.

The triaxial cell is connected to a pressure control system, which is able to fill up the triaxial cell with oil, change the oil pressure during the test, and draining oil from the cell after testing. The pressure control system is described in more detail in **[92.1]**.

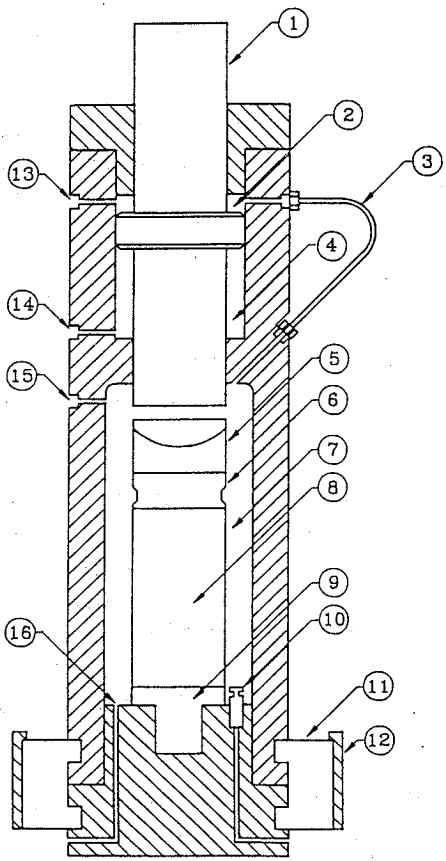

1: Balanced piston
2: Upper oil chamber
3: Connecting oil pipe
4: Lower oil chamber
5: Top cap
6: Top plate (pore pressure outlet)
7: Main oil chamber
8: Concrete specimen
9: Base plate (pore pressure outlet)
10: Electrical outlet
11: Clamp
12: Clamp ring
13: Deairing port A
14: Deairing port B
15: Deairing port C
16: Oil pressure inlet

Fig. 2.1: The triaxial test cell.

The test procedure may be subdivided into three parts. Firstly the preparation of the test specimen, secondly the mounting of the test specimen and finally testing it.

The test specimen is placed inside a rubber membrane in order to avoid oil leaking into the specimen before, during and after the test. The membrane is manufactured by gluing the ends of a rubber sheet together. It is necessary to use at least 3 membranes to avoid an excessive number of failed tests, due to puncturing of the membranes.
The surface of the specimen is sandblasted and brushed with a water based glue in order to expose all voids and microscopic pores at the surface.
In some of the tests, strain gauges are mounted on the specimens. Four strain gauges were mounted, two to measure the longitudinal and two to measure the axial deformation.

Before mounting the specimen, the cylinder is first checked for any holes or voids on the surface. If any holes are found, they are stopped with a quick setting epoxy compound. The strain gauge connections passes out under the rubber membranes and are connected. The cylinder is then placed on the base plate of the triaxial cell, and a heavy duty torque clip is firmly tightened around the rubber and the base plate to form an effective seal. The same is done when connecting the top plate. Then the barrel is lowered down concealing the specimen and the triaxial cell can be filled with oil manually and the test can begin.

The testing and collecting of data is controlled by a program TRIAX, which is described in details in **[92.1]**. Firstly TRIAX increases the hydrostatic stress. Since the oil pressure acts both radially and on top of the cylinder, a hydrostatic stress field is achieved by increasing the oil pressure alone. When the hydrostatic stress field has reached a certain level (equal to the desired side pressure σ_1), TRIAX activates the piston and hereby increases the axial stress σ_3 until failure. During this sequence the volume of the concrete specimen changes which demands a change in oil supply to keep the pressure constant. This is done by manually manipulating the oil supply valves. TRIAX shows whether there is need of oil or too much oil. It is possible after some practice to keep the side pressure within ± 0.3 MPa of the predetermined value.

3 Test results

Four test series were made, two with concrete and two with paste, in which the strength is varied. The tests were performed with normal strength concrete and paste.
In the case of the concrete f_c = 35 MPa for the series B20 and f_c = 52 MPa for the series B40.
For the paste series P40 the compression strength was about f_c = 40 MPa. The low strength series P20 was casted in two batches which resulted in strengths of respectively f_c = 10 MPa and f_c = 14 MPa.

The compressive strength f_c was determined by standard uniaxial compression tests with cylinder specimens (100·200mm²). The triaxial tests were performed on cylinder specimens (100·200mm²).

For the concrete series B20 and B40 the investigation was made for low side pressures only, because in **[92.2]** concrete with high side pressure has already been examined. Therefore only 10 specimens were tested for each concrete series while about 20 for each paste series.

The test program is listed in table 3.1.

	B20	B40	P20	P40
f_c [MPa]	35	52	10/14	40
number	10	10	12/12	19

Table 3.1 *Compressive strength of the test specimens.*

In the following the test data will be presented in σ_1 - σ_3 diagrams. The test data are listed in appendix B.
In figure 3.1 the test series P20 and P40 are presented together with a test series from **[92.2]** where the strength is 70 MPa. Lines through the test points for larger side pressures have been drawn with the inclination coresponding to k=1. It turns out that these lines are intersecting the σ_3-axis at points lying above $-\sigma_3/f_c=1$. This may be interpreted as the uniaxial strength corresponding to high triaxial pressures are higher than the uniaxial strength actually measured. The explanation for this is probably microcracking, the effect of which will disappear when the side pressure is high enough.

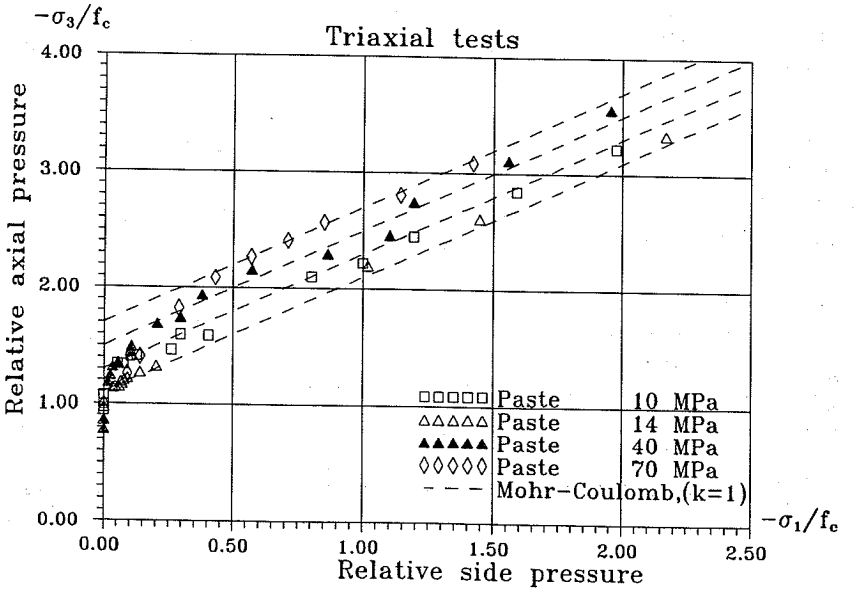

Figure 3.1 *Test data Cement pasta*

In figure 3.2 the transition curves from $-\sigma_3/f_c$ to the Coulomb lines drawn for k=1 are shown.

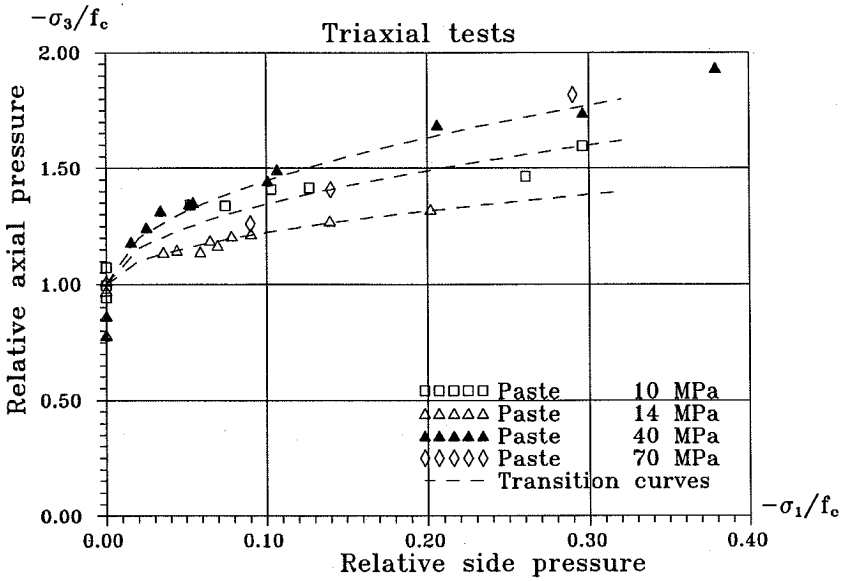

Figure 3.2 *Test data for cement paste small side pressure*

The concrete has only been examined for small side pressures σ_1, because a large test series has already been made for large side pressures **[92.2]**.
The test data for concrete B20 and B40 are shown in figure 3.3. We observe that the triaxial strength σ_3 equals the compression strength f_c for low side pressures in the series B20, meaning that the side pressure doesn't affect the strength. This may be explained by a bleeding effect, see **[87.1]**, which causes the strength of each cylinder to be lower than the strength determined by uniaxial tests.
The tendency of a steeper slope (larger k value) for small side pressures is not as apparent in these test.

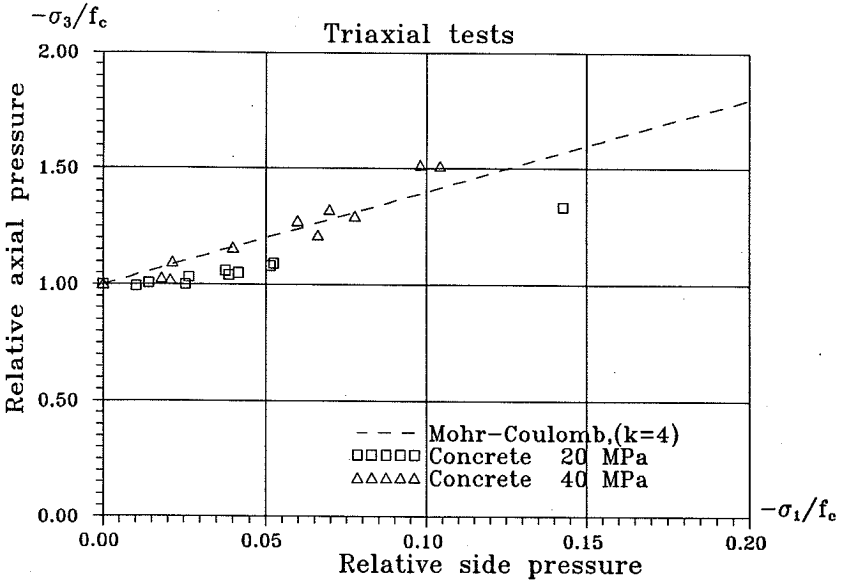

Figure 3.3 *Triaxial Test data for concrete 20 MPa and 40 MPa.*

In some of the P40 and B40 tests strain gauges were mounted on the specimens to measure the lateral and the axial strain. The results are presented in appendix D. The slope of the first part indicates the linear elastic range which can be used to determine Poisons ratio ν. The final part indicates when plastic deformations combined with micro- and macro cracking begin leading finally to fracture. In this range we have larger lateral strains and therefore a steeper slope. If the Coulomb failure condition and normality condition are valid, this slope can be used to determine the k value in the failure criterion, as described in section 1.
In the case of cement paste the fracture phase was so sudden that the strain gauges failed, so in this case it is only possible to determine ν. In the case of concrete the strain gauges did measure part of the fracture range. The lateral strain ϵ_1 versus the axial strain ϵ_3 is shown in figure 3.4.

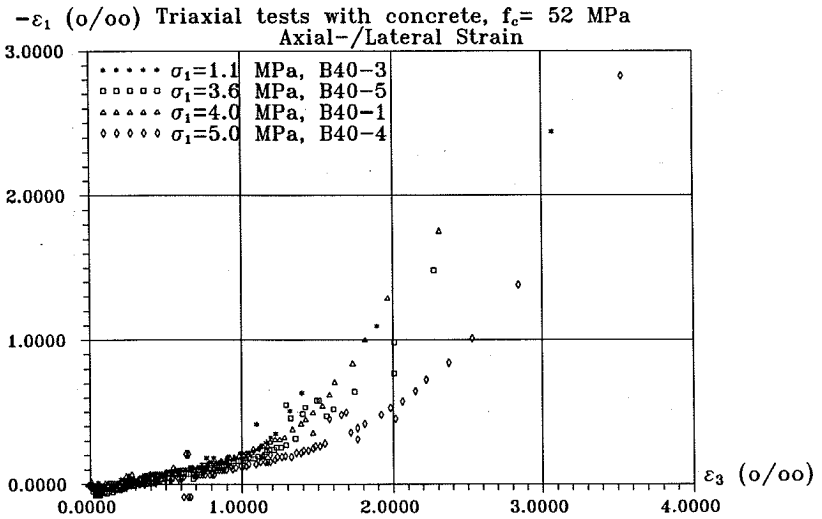

Figure 3.4 *Lateral strain versus axial strain in the concrete tests.*

For a Coulomb material with k = 4 the angle of friction is about $\varphi = 37°$, meaning that the angle of the fracture planes, see figure 1.2, will be about 27°. For a Coulomb material with k = 1 the angle of friction is 0° and the failure angle v is 45°.

This is clearly illustrated in figure 3.5, where $v \approx 45°$ for paste with high side pressures. For low values of side pressure the angle is smaller due to the fact that we are in the transition range having steeper slope than corresponding to k=1.

In appendix E pictures of all the fractured test specimens are presented. The failure angle measured from these pictures are also given in appendix E.

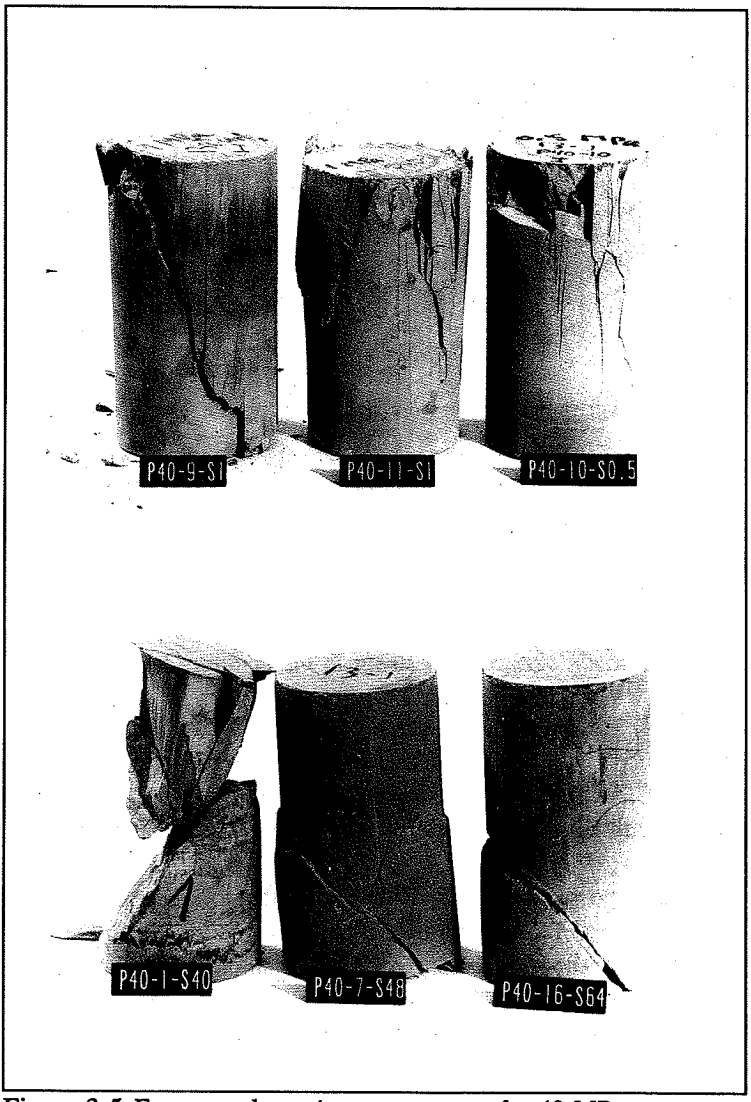

Figure 3.5 *Fracture planes in cement paste f_c=40 MPa.*

Note: In figure 3.5 **Sx.y** indicates a side pressure $\sigma_1 \approx$ x.y MPa

4 Discussion

Having a curved failure criterion it is not possible to define the Coulomb parameters, the angle of friction φ and the cohæsion **c**. However drawing the tangent to the failure curve in a σ - τ - coordinate system or in a σ_1 - σ_3 coordinate system, we may speak about the Coulomb parameters corresponding to this tangent. These may be called the local Coulomb parameters. To determine the σ - τ - curve from the σ_1 - σ_3 - curve, we may use the following relations, which are easely found from Mohr's circle, see figure 4.1.

$$\begin{aligned} \sigma &= \frac{\sigma_1+\sigma_3}{2} + \frac{\sigma_1-\sigma_3}{2}\cdot\cos 2v \\ \tau &= -\frac{\sigma_1-\sigma_3}{2}\cdot\sin 2v \end{aligned} \qquad \textbf{(4.1)}$$

The value of the parameter **k** may be determined by:

$$k = \tan^2(90-v) \qquad \textbf{(4.2)}$$

The value of **k** may also be determined as the slope of the σ_1 - σ_3 - curve. This can be found by using a linear fit based on 3 points. This slope found can be identified as the value of k related to the side pressure of the middle point.

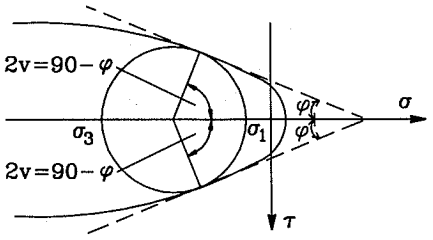

MOHR'S CIRCLE

Figure 4.1

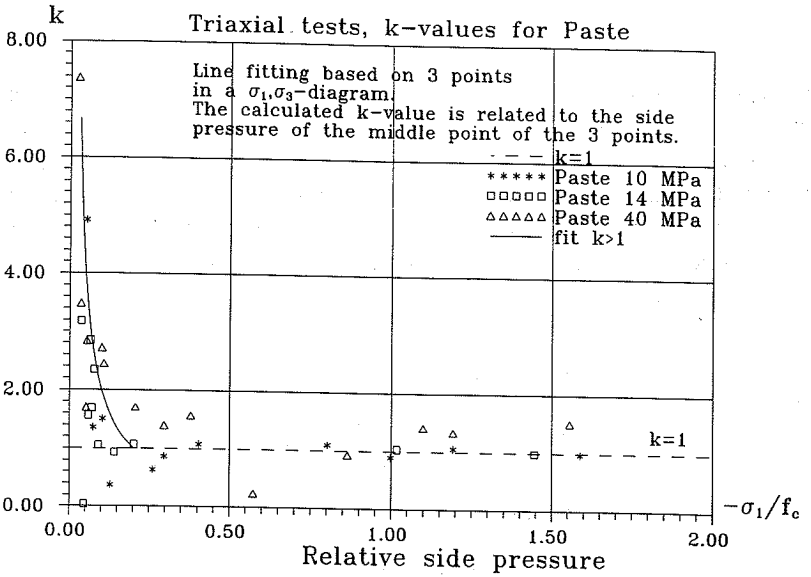

Figure 4.2 *k-values for the paste series.*

For cement paste we find the values shown in figure 4.2. It appears that **k** is very high for low sidepressures, almost 8, and then decreases to 1 when the side pressure is increased to about $0.2f_c$. As a rough estimate we may put

$$\mathbf{k} = \begin{cases} \dfrac{0.2}{\sigma_1/f_c} & \text{for } \sigma_1/f_c < 0.2 \\ 1 & \text{for } \sigma_1/f_c \geq 0.2 \end{cases} \qquad \textbf{(4.3)}$$

Using formula 4.1, 4.2 and 4.3 we may now determine the σ - τ relation for the three paste data set. The calculated data are listed in appendix C and illustrated in figure 4.3.

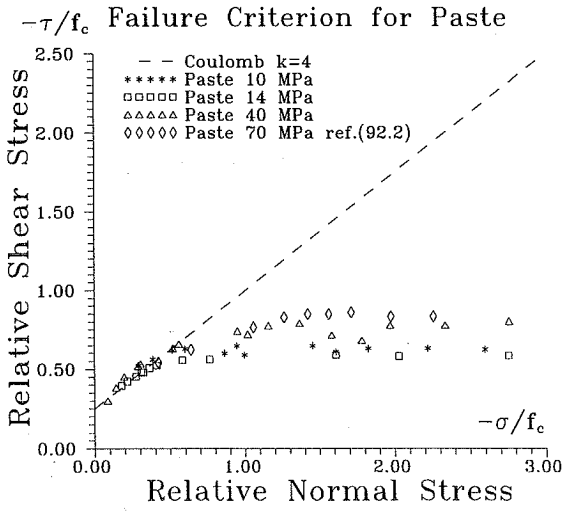

Figure 4.3

It is clearly demonstrated that Coulombs failure condition with k=4 can only be used for cement paste for very small side pressures.

If the same procedure is applied to concrete we find the results shown in figure 4.4. It appears that the scatter of the test data is too large to make a determination of **k** possible.

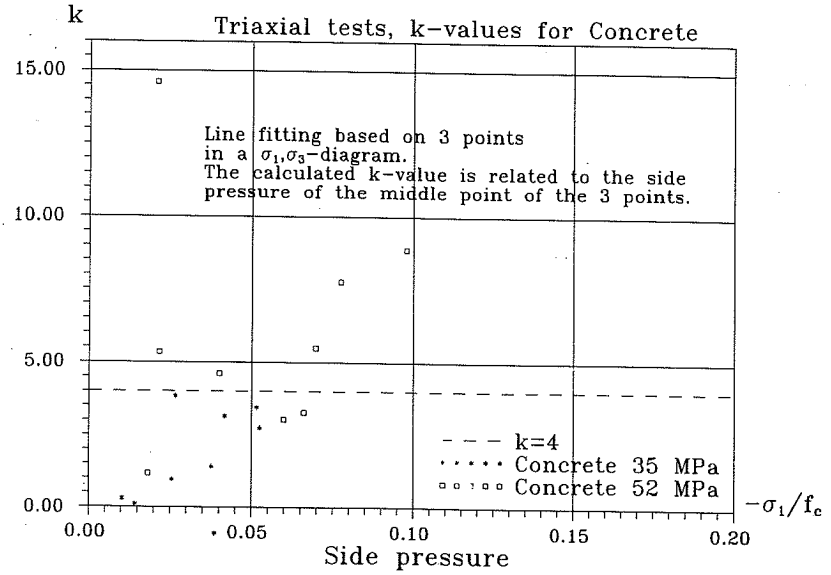

Figure 4.4

If the normality condition is strictly valid it will be possible to determine the k-value by strain measurements as described in section 1. It was only possible to measure a reliable strain in the fracturing range for concrete. In figure 4.5 the lateral strain is shown against the axial strain for specimen B40-1 which had a side pressure σ_1 = 4 MPa.

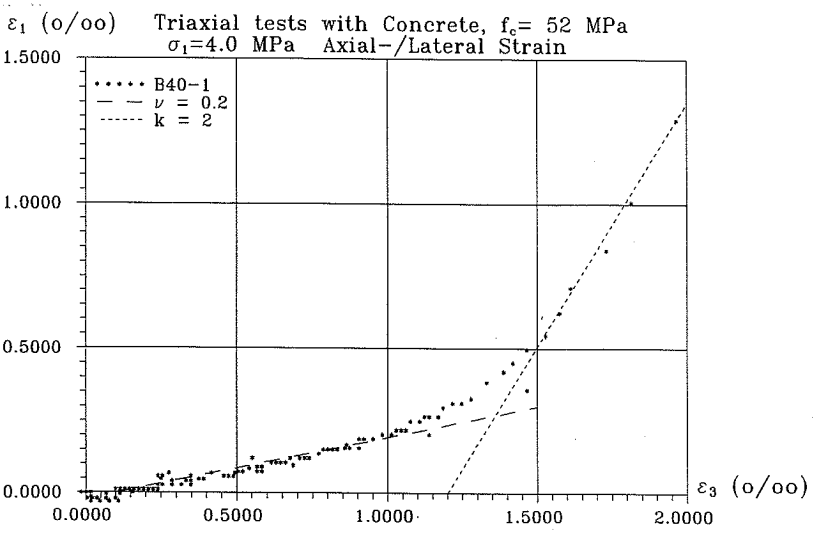

Figure 4.5 *Lateral- versus axial strain in triaxial test with concrete.*

We observe that the slope in the linear elastic range gives approximately $\nu = \Delta\varepsilon_1/\Delta\varepsilon_3 = 0.2$ as expected for concrete, but in the fracture range we get a slope equal to k = 2, i.e. far less than the expected value k = 4, if normality is governing. The explanation is that the strain gauges have failed due to macro cracking before the lateral strain ε_1 reached a sufficiently high level. Further, as mentioned before, the localization of the strains might render the average strains measurements doubtfull. Also the confining effect of the loading plates for applying σ_3 may strongly influence the results. The strain measurements therefore can't be used to measure the k-value in the tests presented in this paper.

Finally we may calculate **k** by measureing the failure angle **v**=45-φ and then use formula (**1.5**). In appendix E the failure angles measured are given and **k** is determined on the basis hereof.
In the case of concrete we observe that k does not differ much from k=4 except in a few cases.
In the case of cement paste with f_c = 40 MPa we observe that the failure angle v increases for small side pressures σ_1 meaning k>4. This confirms the results shown in figure 4.2.

5 Conclusion

The main purpose of this paper is to present some triaxial test results with concrete and cement paste and to examine the failure criterion of these materials. The results obtained have been compared with Coulombs failure criterion and it is indicated that the slope **k** of this failure criterion isn't constant.

For cement paste we may conclude that for high side pressures paste behaves like a Coulomb material with the angle of friction φ equal to zero. For low side pressures the strength is increasing in a higher rate with the side pressure than predicted by Coulombs failure criterion with $\varphi = 0$. It means that the uniaxial strength predicted from triaxial results is higher than the value actually measured by uniaxial tests. It is believed that this is due to microcracking.

For concrete only triaxial strengths for low side pressures have been measured. The scatter of the test results is too big to make any firm conclusion.

It has not been possible to verify the normality condition of perfect plasticity by strain measurements.

The overall conclusion is that neither concrete nor paste can be considered as a Coulomb material. Modifications are necessary in the transition range from uniaxial strength over small side pressures to high side pressures.

Appendix A
Reference list

[87.1] A.M.Neville,J.J.Brooks,*"Concrete Technology"*, Longman Group UK limited, 1987.

[91.1] M.P.Nielsen,L.Pilegaard Hansen,A.Rathkjen,*"Rumlige Spændings- og Deformationstilstande"*, Mekanik 2.2, del 1 og 2. Aalborg 1991.

[92.1] Kaare.K.B.Dahl,*"The Calibration and Use of a Triaxial Cell"*,Ph.d-thesis, R285, ABK, Technical University of Denmark. 1992.

[92.2] Kaare.K.B.Dahl,*"A Failure Criterion for Normal and High Strength Concrete"*,Ph.d-thesis, R286, ABK, Technical University of Denmark. 1992.

[92.3] Kaare.K.B.Dahl,*"A Constitutive Model for Normal and High Strength Concrete"*,Ph.d-thesis, R287, ABK, Technical University of Denmark. 1992.

[93.1] R.A.Vonk,*"A Micromechanical Investigation of Softening of Concrete Loaded in Compression"*,Heron, Vol.38, no.3, 1993.

Appendix B
Test Data

Triaxial tests with concrete f_c = 35 MPa and 52 MPa.

σ_3/f_c	σ_3/f_c	Cylinder, f_c (MPa)		P_{peak} (kN)	σ_1 (MPa) at peak	σ_3' (MPa) $=P_{peak}/A_{cyl}$	σ_1 (MPa) $=\sigma_3'+\sigma_1$
0.0103	0.9941	B20-7	34.51	266.642	0.3551	33.95	34.31
0.0142	1.0072	B20-6	34.51	269.120	0.4904	34.27	34.76
0.0255	0.9993	B20-5	34.51	263.939	0.8793	33.61	34.49
0.0265	1.0332	B20-9	34.51	270.760	0.9133	34.75	35.66
0.0377	1.0593	B20-8	34.51	276.880	1.3024	35.25	36.56
0.0387	1.0422	B20-4	34.51	272.020	1.3360	34.63	35.97
0.0417	1.0512	B20-10	34.51	273.640	1.4376	34.84	36.28
0.0515	1.0822	B20-2	34.51	279.406	1.7760	35.58	37.35
0.0524	1.0903	B20-3	34.51	281.309	1.8096	35.82	37.63
0.1427	1.3331	B20-1	34.51	322.686	4.924	41.09	46.01
0.0182	1.027	B40-9	52.0	412.017	0.9467	52.46	53.41
0.0208	1.020	B40-10	52.0	408.066	1.08197	51.96	53.04
0.0215	1.097	$B40\text{-}3_{sg}$	52.0	439.331	1.1159	55.93	57.05
0.0400	1.157	$B40\text{-}2_{sg}$	52.0	456.330	2.080	58.10	60.18
0.0598	1.273	B40-7	52.0	495.493	3.111	63.09	66.20
0.0660	1.212	B40-8	52.0	468.216	3.432	59.62	63.05
0.0696	1.321	$B40\text{-}5_{sg}$	52.0	510.928	3.619	65.05	68.67
0.0774	1.294	$B40\text{-}1_{sg}$	52.0	496.943	4.024	63.27	67.30
0.0979	1.518	$B40\text{-}4_{sg}$	52.0	579.865	5.092	73.83	78.92
0.1041	1.512	B40-6	52.0	575.071	5.411	73.22	78.63

Triaxial tests with cement paste f_c = 10 MPa and 14 MPa.

σ_1/f_c	σ_3/f_c	Cylinder, f_c (MPa)		P_{peak} (kN)	σ_1 (MPa) at peak	σ_3' (MPa) $=P_{peak}/A_{cyl}$	σ_3 (MPa) $=\sigma_3'+\sigma_1$
0.0524	1.343	P10-9	10.0	101.362	0.5242	12.91	13.43
0.0744	1.339	P10-8	10.0	99.350	0.7440	12.65	13.39
0.1032	1.409	P10-7	10.0	102.553	1.032	13.06	14.09
0.1268	1.416	P10-10	10.0	101.268	1.268	12.89	14.16
0.2605	1.466	P10-6	10.0	94.685	2.605	12.06	14.66
0.296	1.595	P10-12	10.0	102.013	2.959	12.99	15.95
0.404	1.588	P10-5	10.0	92.987	4.042	11.84	15.88
0.802	2.102	P10-4	10.0	102.140	8.016	13.00	21.02
0.998	2.220	P10-11	10.0	96.002	9.976	12.22	22.20
1.192	2.454	P10-3	10.0	99.127	11.92	12.62	24.54
1.588	2.851	P10-2	10.0	99.161	15.88	12.63	28.51
1.975	3.223	P10-1	10.0	97.958	19.75	12.47	32.23
0.0355	1.139	P14-15	13.82	119.792	0.4904	15.25	15.74
0.0440	1.147	P14-16	13.82	119.789	0.6087	15.25	15.86
0.0587	1.141	P14-17	13.82	117.504	0.8120	14.96	15.77
0.0648	1.189	P14-21	13.82	122.116	0.8963	15.55	16.44
0.0697	1.170	P14-14	13.82	119.419	0.9639	15.20	16.17
0.0783	1.207	P14-18	13.82	122.587	1.082	15.61	16.69
0.0905	1.220	P14-22	13.82	122.673	1.251	15.62	16.87
0.1395	1.272	P14-13	13.82	122.948	1.928	15.65	17.58
0.202	1.324	P14-23	13.82	121.844	2.790	15.51	18.31
1.017	2.200	P14-24	13.82	128.447	14.06	16.35	30.41
1.446	2.612	P14-20	13.82	126.574	19.99	16.12	36.11
2.170	3.338	P14-19	13.82	126.764	30.00	16.14	46.14

Triaxial tests with cement paste f_c = 40 MPa.

σ_1/f_c	σ_3/f_c	Cylinder, f_c (MPa)	P_{peak} (kN)	σ_1 (MPa) at peak	σ_3' (MPa) $=P_{peak}/A_{cyl}$	σ_3 (MPa) $=\sigma_3'+\sigma_1$
0	0.782	P40-18$_{sg}$ 41.23	251.745	0	32.22	32.22
0	0.864	P40-17$_{sg}$ 41.23	279.213	0	35.60	35.60
0.0154	1.183	P40-10 40.54	371.673	0.6255	47.32	47.95
0.0250	1.245	P40-11 40.54	388.396	1.014	49.45	50.46
0.0338	1.317	P40-9 40.54	408.732	1.370	52.04	53.41
0.0486	1.216	P40-19$_{sg}$ 44.54	408.163	2.166	51.97	54.14
0.0517	1.347	P40-12 40.54	412.313	2.096	52.50	54.60
0.0542	1.353	P40-8 40.54	413.454	2.199	52.64	54.84
0.101	1.446	P40-6 40.18	424.192	4.074	54.01	58.08
0.1068	1.493	P40-13 40.89	445.007	4.365	56.66	61.03
0.206	1.689	P40-5 42.46	494.535	8.726	62.97	71.70
0.296	1.741	P40-15 40.89	463.910	12.10	59.07	71.17
0.379	1.936	P40-4 42.17	515.394	16.00	65.62	81.62
0.573	2.158	P40-3 42.17	524.910	24.18	66.83	91.01
0.863	2.298	P40-2 37.18	418.878	32.09	53.33	85.42
1.099	2.464	P40-1 36.66	424.666	40.27	54.07	90.34
1.192	2.749	P40-7 40.18	491.370	47.89	62.56	110.45
1.556	3.114	P40-16 41.23	504.246	64.16	64.2	128.36
1.954	3.562	P40-14 40.89	516.245	79.90	65.73	145.63

Appendix C
k - values

This appendix contains the calculated k-values on basis of formula (4.2)

Paste 10 MPa		Paste 14 MPa		Paste 40 MPa	
σ_1/f_c	k	σ_1/f_c	k	σ_1/f_c	k
0.05242	4.918	0.0355	3.182	0.025	7.3712
0.0744	1.358	0.044	0.035	0.0338	3.4817
0.1032	1.503	0.0587	1.564	0.0517	1.7001
0.12682	0.366	0.0648	2.847	0.0542	2.8358
0.2605	0.635	0.0697	1.688	0.1068	2.4437
0.29591	0.87	0.0783	2.342	0.101	2.7165
0.4042	1.081	0.0905	1.051	0.206	1.7098
0.8016	1.098	0.1395	0.932	0.296	1.3987
0.9976	0.901	0.2018	1.065	0.379	1.5665
1.192	1.059	1.017	1.04	0.573	0.2414
1.588	0.982	1.446	0.988	0.863	0.9289
-	-	-	-	1.192	1.3378
-	-	-	-	1.556	1.5142
-	-	-	-	1.099	1.4112

Appendix D
Strain diagrams

This appendix contains the test data from the strain gauge measurements. They are presented in two diagrams, fistly σ_3 versus the lateral strain ϵ_1 and the axial strain ϵ_3 and secondly the lateral strain versus the axial strain.
Strain gauges was mounted on P40-17,P40-18,P40-19,B40-1,B40-2,B40-3, B40-4 and B40-5.

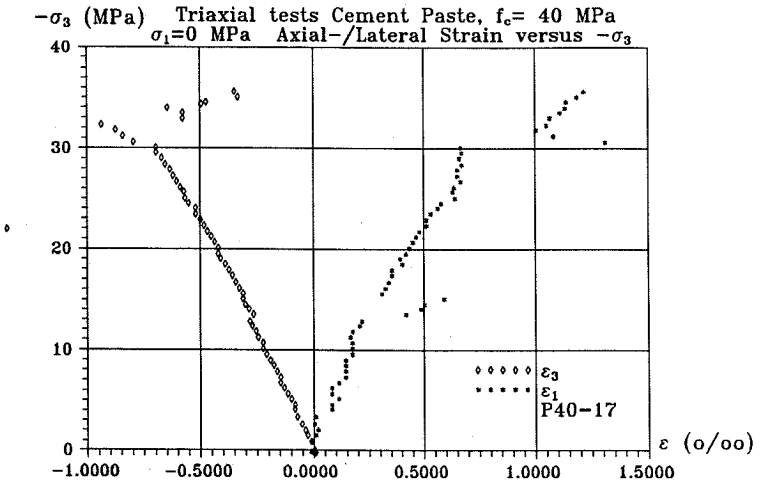
$-\sigma_3$ (MPa) Triaxial tests Cement Paste, f_c= 40 MPa
σ_1=0 MPa Axial-/Lateral Strain versus $-\sigma_3$
40
30
20
10
0
−1.0000
−0.5000
0.0000
0.5000
1.0000
1.5000
ε_3
ε_1
P40-17
ε (o/oo)

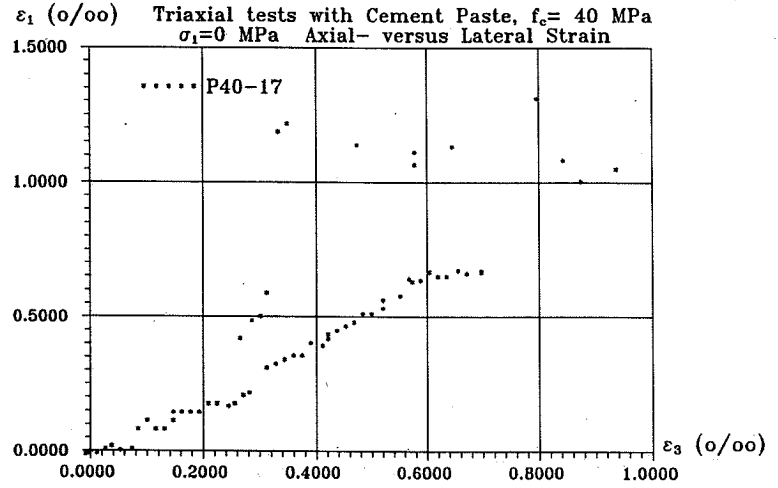
ε_1 (o/oo) Triaxial tests with Cement Paste, f_c= 40 MPa
σ_1=0 MPa Axial- versus Lateral Strain
1.5000
1.0000
0.5000
0.0000
P40-17
0.0000
0.2000
0.4000
0.6000
0.8000
1.0000
ε_3 (o/oo)

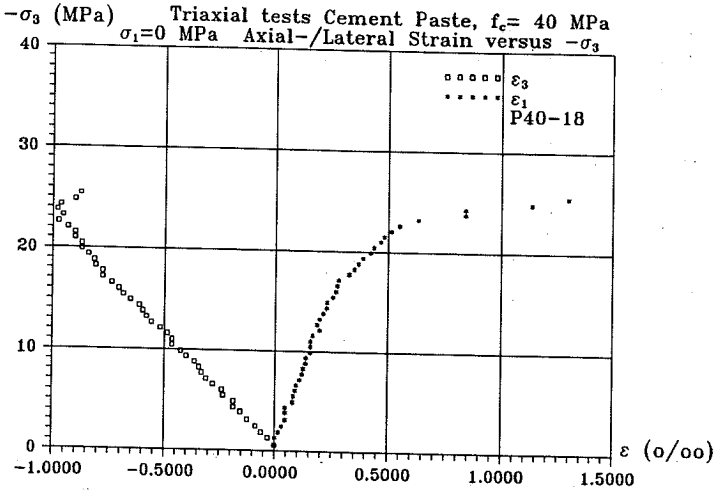
$-\sigma_3$ (MPa)
Triaxial tests Cement Paste, f_c= 40 MPa
σ_1=0 MPa Axial-/Lateral Strain versus $-\sigma_3$
ε_3
ε_1
P40-18
40
30
20
10
0
-1.0000
-0.5000
0.0000
0.5000
1.0000
1.5000
ε (o/oo)

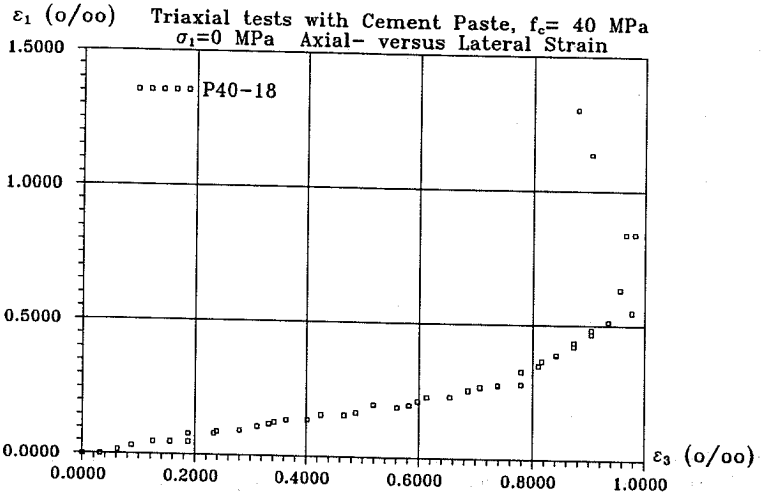
ε_1 (o/oo)
Triaxial tests with Cement Paste, f_c= 40 MPa
σ_1=0 MPa Axial- versus Lateral Strain
P40-18
1.5000
1.0000
0.5000
0.0000
0.0000
0.2000
0.4000
0.6000
0.8000
1.0000
ε_3 (o/oo)

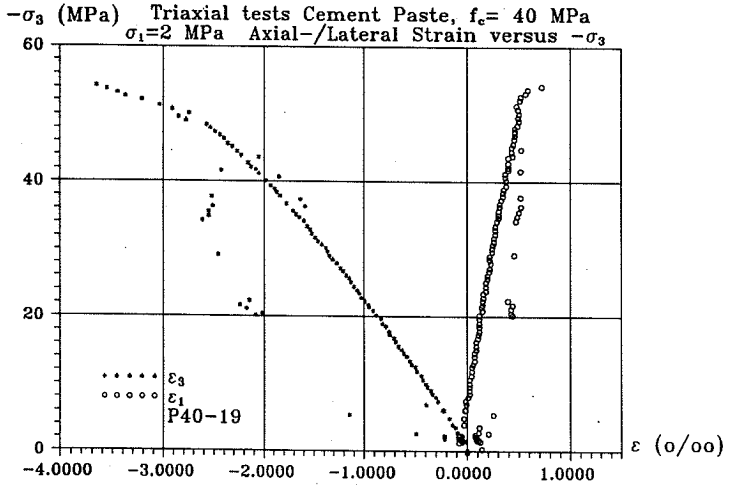
−σ3 (MPa) Triaxial tests Cement Paste, fc= 40 MPa
σ1=2 MPa Axial−/Lateral Strain versus −σ3
60
40
20
0
ε3
ε1
P40−19
−4.0000
−3.0000
−2.0000
−1.0000
0.0000
1.0000
ε (o/oo)

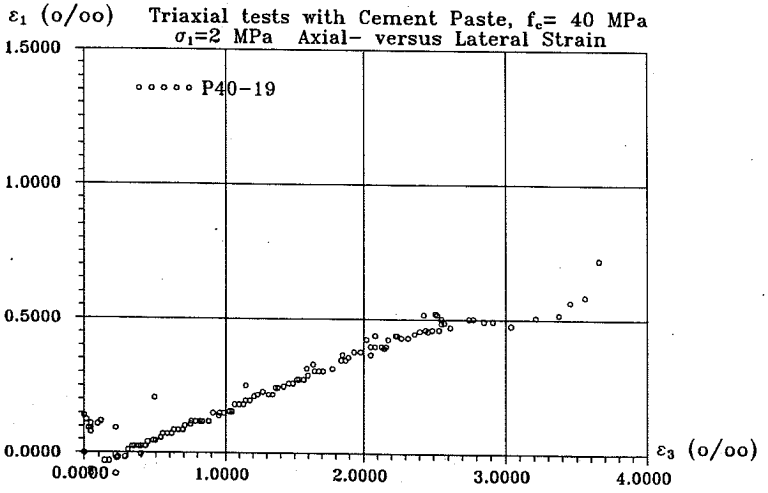
ε1 (o/oo) Triaxial tests with Cement Paste, fc= 40 MPa
σ1=2 MPa Axial− versus Lateral Strain
1.5000
1.0000
0.5000
0.0000
P40−19
0.0000
1.0000
2.0000
3.0000
4.0000
ε3 (o/oo)

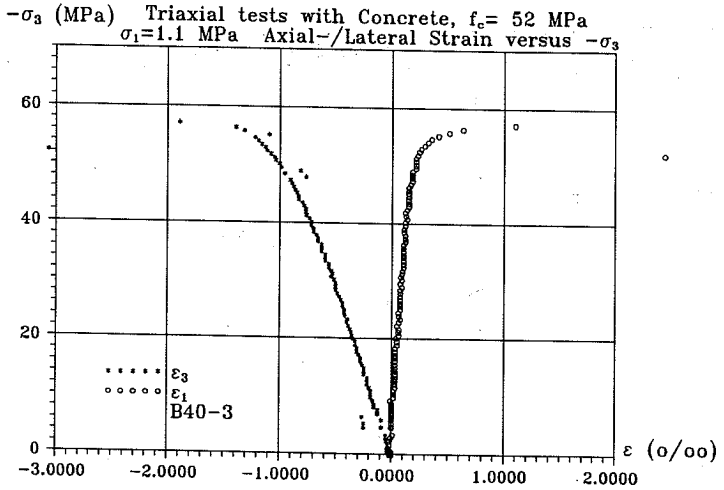
$-\sigma_3$ (MPa) Triaxial tests with Concrete, f_c= 52 MPa
σ_1=1.1 MPa Axial-/Lateral Strain versus $-\sigma_3$
60
40
20
0
ε_3
ε_1
B40-3
-3.0000
-2.0000
-1.0000
0.0000
1.0000
2.0000
ε (o/oo)

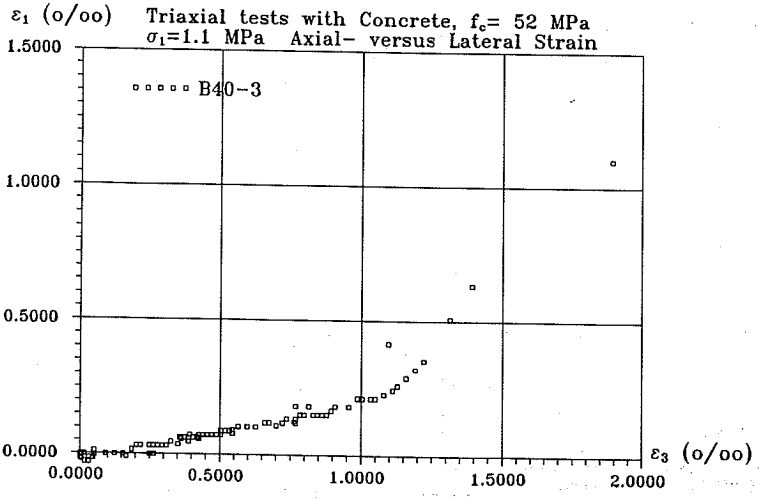
ε_1 (o/oo) Triaxial tests with Concrete, f_c= 52 MPa
σ_1=1.1 MPa Axial- versus Lateral Strain
1.5000
1.0000
0.5000
0.0000
B40-3
0.0000
0.5000
1.0000
1.5000
2.0000
ε_3 (o/oo)

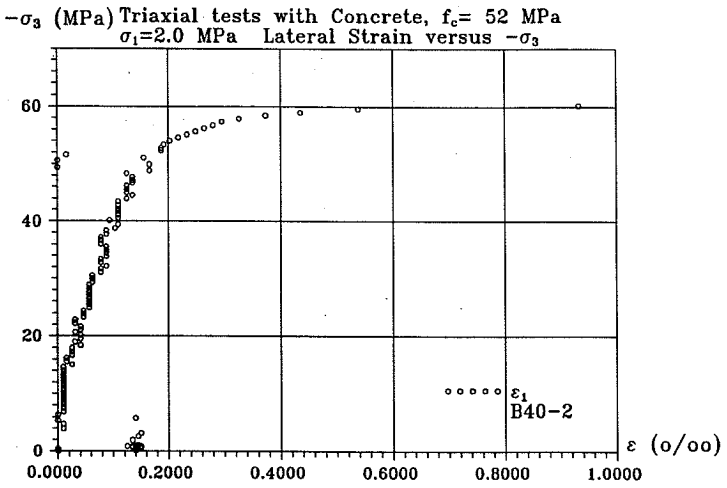
$-\sigma_3$ (MPa) Triaxial tests with Concrete, f_c= 52 MPa
σ_1=2.0 MPa Lateral Strain versus $-\sigma_3$
60
40
20
0
0.0000
0.2000
0.4000
0.6000
0.8000
1.0000
ε_1
B40-2
ε (o/oo)

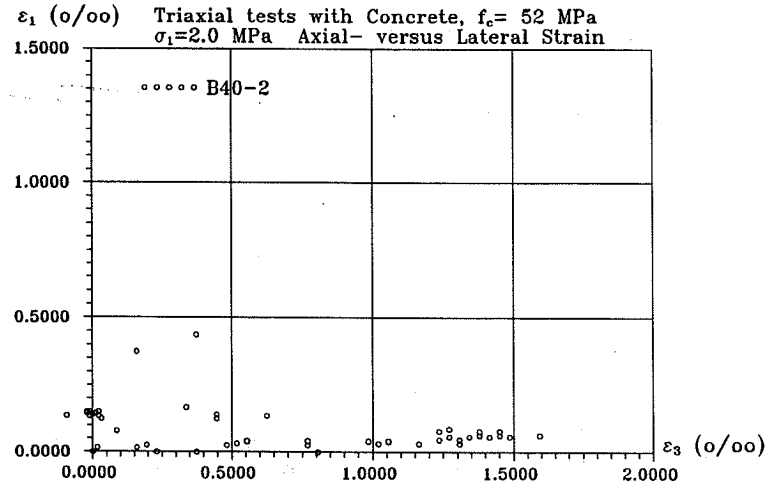
ε_1 (o/oo) Triaxial tests with Concrete, f_c= 52 MPa
σ_1=2.0 MPa Axial- versus Lateral Strain
1.5000
1.0000
0.5000
0.0000
B40-2
0.0000
0.5000
1.0000
1.5000
2.0000
ε_3 (o/oo)

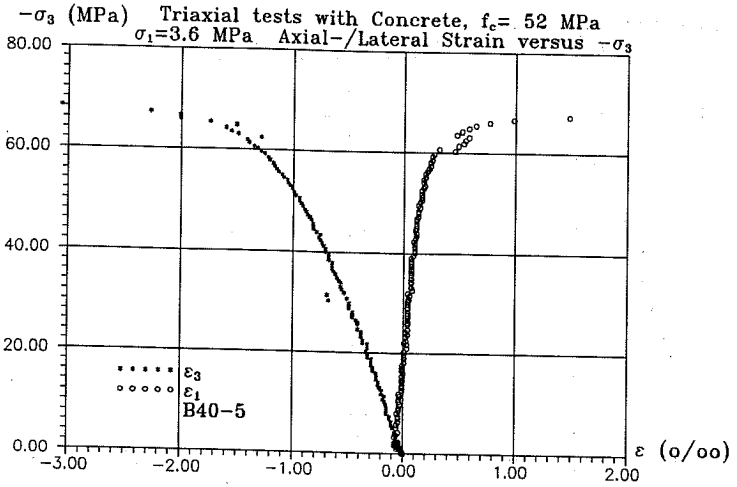
$-\sigma_3$ (MPa) Triaxial tests with Concrete, f_c= 52 MPa
σ_1=3.6 MPa Axial-/Lateral Strain versus $-\sigma_3$
80.00
60.00
40.00
20.00
0.00
-3.00
-2.00
-1.00
0.00
1.00
2.00
ε (o/oo)
ε_3
ε_1
B40-5

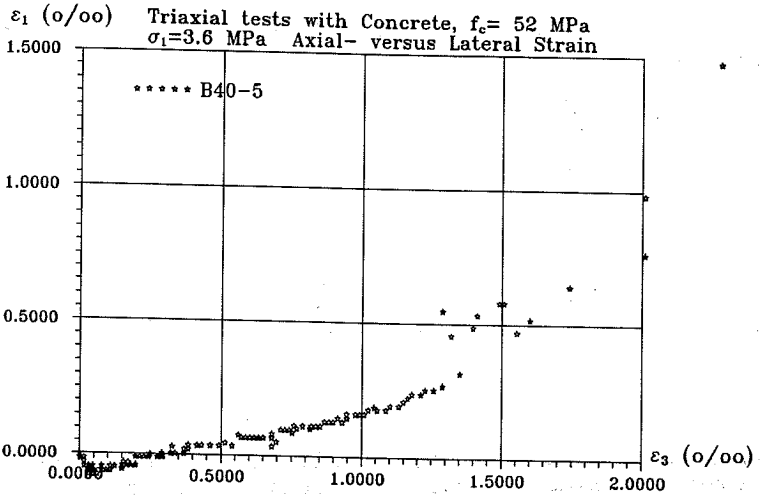
ε_1 (o/oo) Triaxial tests with Concrete, f_c= 52 MPa
σ_1=3.6 MPa Axial- versus Lateral Strain
1.5000
1.0000
0.5000
0.0000
0.0000
0.5000
1.0000
1.5000
2.0000
ε_3 (o/oo)
B40-5

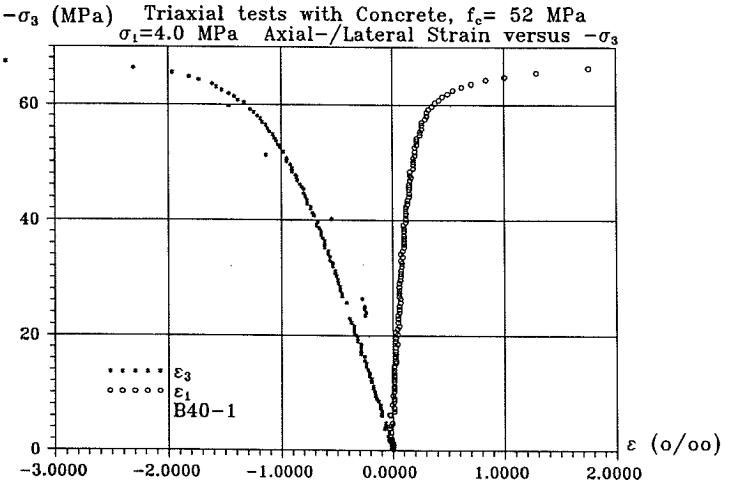
$-\sigma_3$ (MPa) Triaxial tests with Concrete, f_c= 52 MPa
σ_1=4.0 MPa Axial-/Lateral Strain versus $-\sigma_3$
60
40
20
0
ε_3
ε_1
B40-1
-3.0000
-2.0000
-1.0000
0.0000
1.0000
2.0000
ε (o/oo)

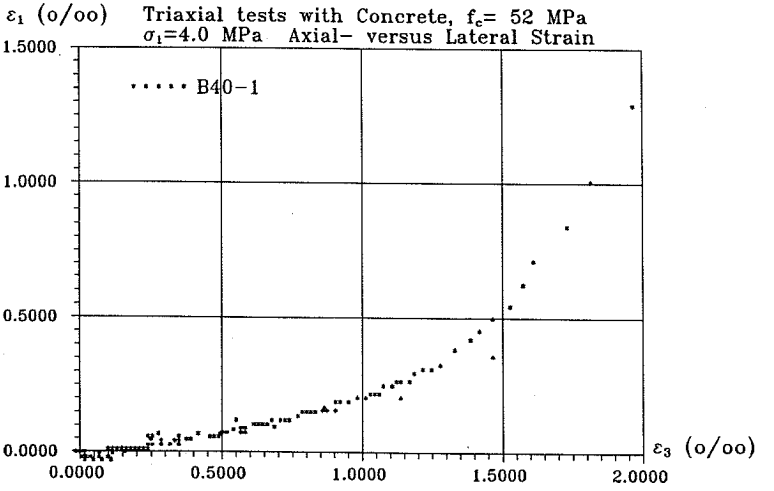
ε_1 (o/oo) Triaxial tests with Concrete, f_c= 52 MPa
σ_1=4.0 MPa Axial- versus Lateral Strain
1.5000
1.0000
0.5000
0.0000
B40-1
0.0000
0.5000
1.0000
1.5000
2.0000
ε_3 (o/oo)

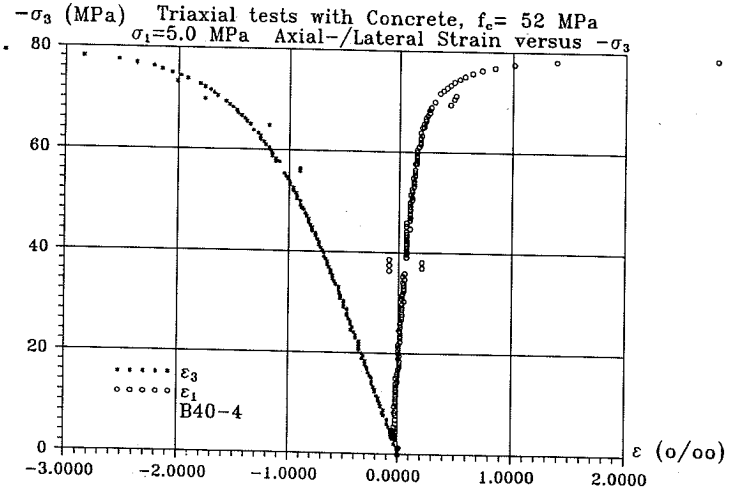
$-\sigma_3$ (MPa) Triaxial tests with Concrete, f_c= 52 MPa
σ_1=5.0 MPa Axial-/Lateral Strain versus $-\sigma_3$
80
60
40
20
0
ε_3
ε_1
B40-4
-3.0000
-2.0000
-1.0000
0.0000
1.0000
2.0000
ε (o/oo)

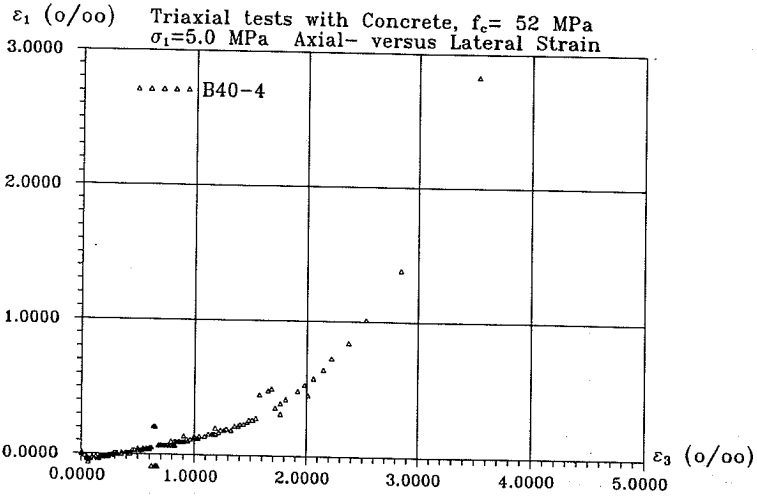
ε_1 (o/oo) Triaxial tests with Concrete, f_c= 52 MPa
σ_1=5.0 MPa Axial- versus Lateral Strain
3.0000
2.0000
1.0000
0.0000
B40-4
0.0000
1.0000
2.0000
3.0000
4.0000
5.0000
ε_3 (o/oo)

Appendix E
Picture of test specimens

This appendix contains pictures and measured failure angles v.

Triaxial tests with concrete f_c = 35 MPa and 52 MPa

σ_1/f_c	σ_3/f_c	Cylinder, f_c (MPa)		v	φ= 90-2v	k=tan²(45+φ/2)
0.0103	0.9941	B20-7	34.51	25	40	4.60
0.0142	1.0072	B20-6	34.51	15	60	13.93
0.0255	0.9993	B20-5	34.51	20	50	7.55
0.0265	1.0332	B20-9	34.51	26	38	4.20
0.0377	1.0593	B20-8	34.51	26	38	4.20
0.0387	1.0422	B20-4	34.51	28	34	3.54
0.0417	1.0512	B20-10	34.51	26.5	37	4.0
0.0515	1.0822	B20-2	34.51	26.5	37	4.0
0.0524	1.0903	B20-3	34.51	26.5	37	4.0
0.1427	1.3331	B20-1	34.51	26.5	37	4.0
0.0182	1.027	B40-9	52.0	26.5	37	4.0
0.0208	1.020	B40-10	52.0	*	*	>>4
0.0215	1.097	B40-3_{rg}	52.0	*	*	>>4
0.0400	1.157	B40-2_{rg}	52.0	-	-	-
0.0598	1.273	B40-7	52.0	26.5	37	4.0
0.0660	1.212	B40-8	52.0	26.5	37	4.0
0.0696	1.321	B40-5_{rg}	52.0	26.5	37	4.0
0.0774	1.294	B40-1_{rg}	52.0	26.5	37	4.0
0.0979	1.518	B40-4_{rg}	52.0	26.5	37	4.0
0.1041	1.512	B40-6	52.0	26.5	37	4.0

Triaxial tests with cement paste f_c = 10 MPa samt 14 MPa.

σ_1/f_c	σ_3/f_c	Cylinder,	f_c (MPa)	v	φ= 90-2v	k=tan²(45+φ/2)
0.0524	1.343	P10-9	10.0	26.5	37	4.0
0.0744	1.339	P10-8	10.0	30	30	3.0
0.1032	1.409	P10-7	10.0	26.5	37	4.0
0.1268	1.416	P10-10	10.0	26.5	37	4.0
0.2605	1.466	P10-6	10.0	26.5	37	4.0
0.296	1.595	P10-12	10.0	26.5	37	4.0
0.404	1.588	P10-5	10.0	26.5	37	4.0
0.802	2.102	P10-4	10.0	26.5	37	4.0
0.998	2.220	P10-11	10.0	26.5	37	4.0
1.192	2.454	P10-3	10.0	35	20	2.0
1.588	2.851	P10-2	10.0	26.5	37	4.0
1.975	3.223	P10-1	10.0	26.5	37	4.0
0.0355	1.139	P14-15	13.82	26.5	37	4.0
0.0440	1.147	P14-16	13.82	22	46	6.13
0.0587	1.141	P14-17	13.82	40	10	1.42
0.0648	1.189	P14-21	13.82	26.5	37	4.0
0.0697	1.170	P14-14	13.82	35	20	2.0
0.0783	1.207	P14-18	13.82	26.5	37	4.0
0.0905	1.220	P14-22	13.82	35	20	2.0
0.1395	1.272	P14-13	13.82	35	20	2.0
0.202	1.324	P14-23	13.82	35	20	2.0
1.017	2.200	P14-24	13.82	40	10	1.42
1.446	2.612	P14-20	13.82	30	30	3.0
2.170	3.338	P14-19	13.82	35	20	2.0

Triaxial tests with cement paste f_c = 40 MPa.

σ_1/f_c	σ_3/f_c	Cylinder, f_c (MPa)		v	φ = 90–2v	$k=\tan^2(45+\varphi/2)$
0	0.782	P40-18$_{sg}$	41.23	*	*	>>4
0	0.864	P40-17$_{sg}$	41.23	*	*	>>4
0.0154	1.183	P40-10	40.54	20	50	7.5
0.0250	1.245	P40-11	40.54	20	50	7.5
0.0338	1.317	P40-9	40.54	20	50	7.5
0.0486	1.216	P40-19$_{sg}$	44.54	-	-	-
0.0517	1.347	P40-12	40.54	-	-	-
0.0542	1.353	P40-8	40.54	30	30	3.0
0.101	1.446	P40-6	40.18	26.5	37	4.0
0.1068	1.493	P40-13	40.89	26.5	37	4.0
0.206	1.689	P40-5	42.46	26.5	37	4.0
0.296	1.741	P40-15	40.89	26.5	37	4.0
0.379	1.936	P40-4	42.17	45	0	1.0
0.573	2.158	P40-3	42.17	45	0	1.0
0.863	2.298	P40-2	37.18	40	10	1.42
1.099	2.464	P40-1	36.66	45	0	1.0
1.192	2.749	P40-7	40.18	45	0	1.0
1.556	3.114	P40-16	41.23	45	0	1.0
1.954	3.562	P40-14	40.89	45	0	1.0

Test specimens from series B20 ($f_c \approx 35$MPa) and B40 ($f_c \approx 52$MPa).

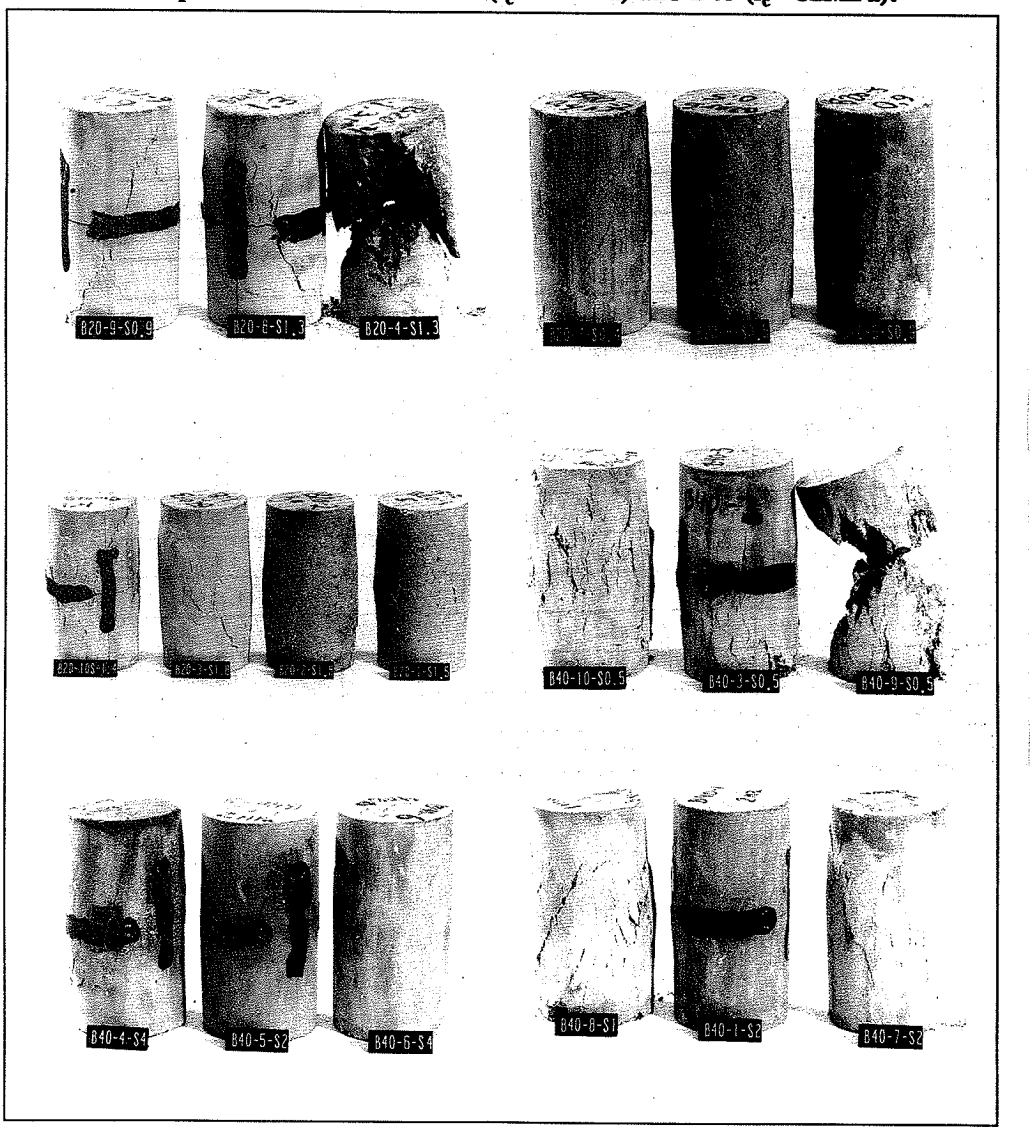

Test specimens from series P20 ($f_c \approx 10$MPa).

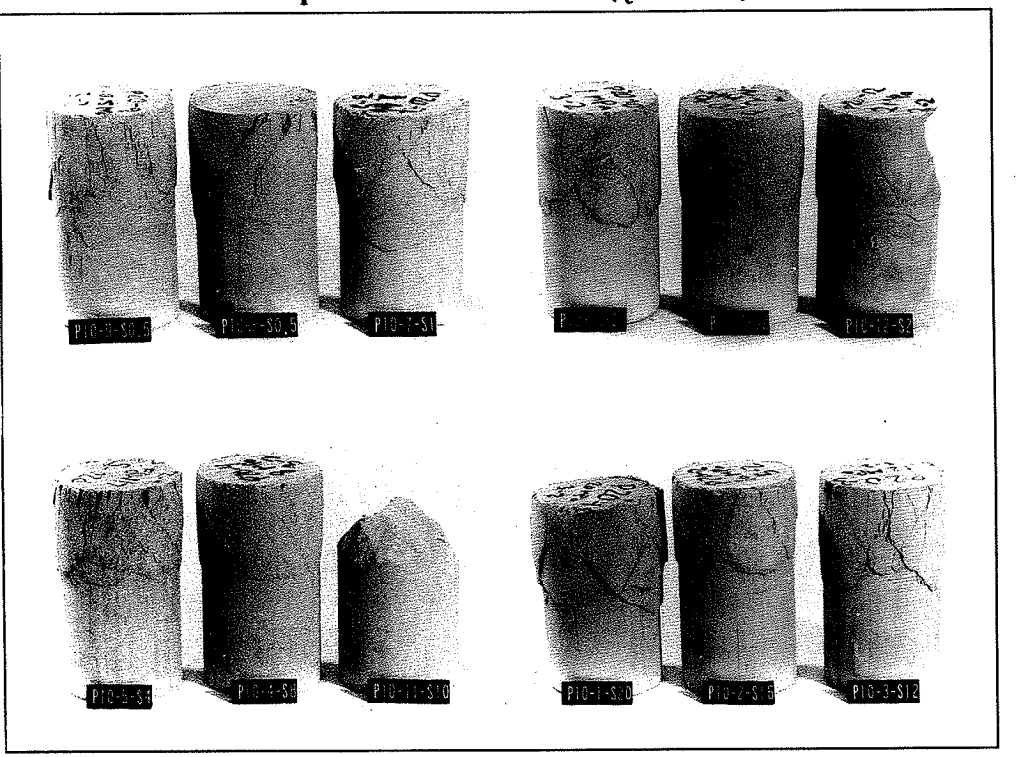

Test specimens from series P20 ($f_c \approx 14$MPa).

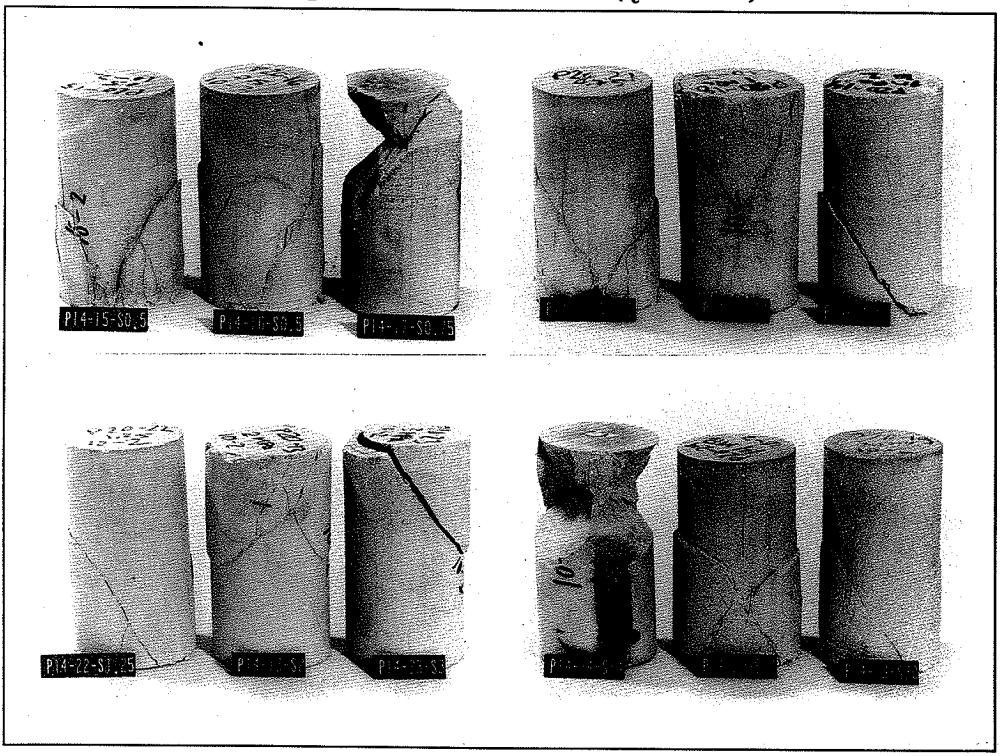

Test specimens from series P40 ($f_c \approx 40$MPa).

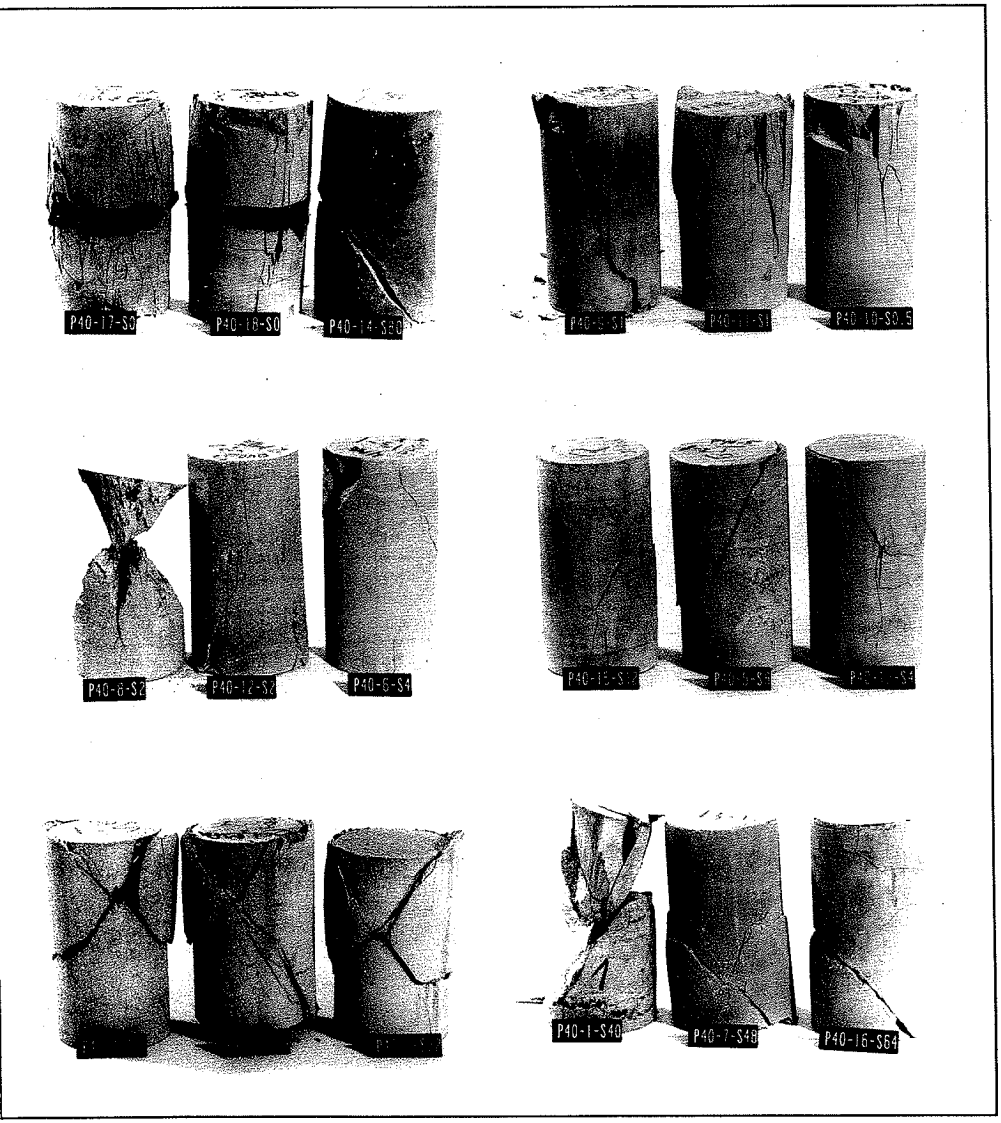

Appendix F

Mix proportions

This appendix contains the mix proportions of the four tested materials P20,P40, B20 and B40.

kg/m³	P20	P40	B20	B40
Cement	637	867	170	260
Fly ash	280	133	75	40
MS-slurry	-	120	-	36
Water	637	500	170	163
Sand (0-4 mm)	-	-	618	600
Gravelit (4-8 mm)	-	-	245	257
Granit (4-16 mm)	-	-	977	1026
Conplast 212	-	4.7	-	1.34

AFDELINGEN FOR BÆRENDE KONSTRUKTIONER
DANMARKS TEKNISKE UNIVERSITET

Department of Structural Engineering
Technical University of Denmark, DK–2800 Lyngby

SERIE R
(Tidligere: Rapporter)

R 296. IBSØ, JAN BEHRENDT & RASMUSSEN, LARS JUEL: Vridning af armerede normal– og højstyrkebetonbjælker. 1992.
R 297. RIBERHOLT, HILMER, JOHANNESEN, JOHANNES MORSING & RASMUSSEN, LARS JUEL: Rammehjørner med indlimede stålstænger i limtræ. 1992.
R 298. JENSEN, RALPH BO: Modified Finite Element Method modelling Fracture Mechanical Failure in wooden beams. 1992.
R 299. IBSØ, JAN BEHRENDT & AGERSKOV, HENNING: Fatigue Life of Offshore Steel Structures under Stochastic Loading. 1992.
R 300. HANSEN, SVEND OLE: Reliability of Wind Loading on Low–Rise Buildings in a Group. 1992.
R 301. AARRE, TINE: Tensile characteristics of FRC with special emphasis on its applicability in a continuous pavement. 1992.
R 302. GLAVIND, METTE: Evaluation of the Compressive Behaviour of Fiber Reinforced High Strength Concrete. 1992.
R 303. NIELSEN, LEIF OTTO: A C ++ basis for computational mechanics software. 1993
R 304. Resuméoversigt 1992 – Summaries of Papers 1992.
R 305. HANSEN, SØREN, STANG, HENRIK: Eksperimentelt bestemte mekaniske egenskaber for fiberbeton. 1993.
R 306. NIELSEN, PER KASTRUP, ELGAARD JENSEN, HENRIK, SCHMIDT, CLAUS, NIELSEN, M.P.: Forskydning i armerede teglbjælker. 1993.
R 307. CHRISTOFFERSEN, JENS, JAGD, LARS, NIELSEN, M.P.: HOTCH-POTCH Pladeelementet – Finite element til beregning af armerede betonplader. 1993.
R 308. NIELSEN, LEIF OTTO: A C++ class library for FEM special purpose software. 1994.
R 309. DULEVSKI, ENCHO M.: Global Structural Analysis of Steel Box Girder Bridges for Various Loads. 1994.
R 310. Resuméoversigt 1993 – Summaries of Papers 1993.
R 311. JIN–PING ZHANG: Strength of Cracked Concrete. Part 1 – Shear Strength of Conventional Reinforced Concrete Beams, Deep Beams, Corbels, and Prestressed Reinforced Concrete Beams without Shear Reinforcement. 1994.
R 312. OLSEN, DAVID HOLKMANN: Fracture of Concrete A Test Series. 1994.
R 313. OLSEN, DAVID HOLKMANN: Fracture of Concrete A Test Series Appendix I. 1994.
R 314. DAHL, KAARE K.B.: Construction Joints in Normal and High Strength Concrete. 1994.
R 315. KARLSHØJ, JAN: Principper og metoder for opstilling af datamodeller til byggetekniske anvendelser. 1994.
R 316. HANSEN, THOMAS CORNELIUS: Fatigue and Crack Propagation. A new approach to predict crack propagation behavior. 1994.
R 317. JAGD, LARS, CHRISTOFFERSEN, JENS, NIELSEN, M.P.: The HOTCH–POTCH Disk Element – Finite Element for Analysis of Reinforced Concrete Disks. 1994.
R 318. JAGD, LARS, CHRISTOFFERSEN, JENS, NIELSEN, M.P.: The HOTCH–POTCH Disk Element – Finite Element for Analysis of Reinforced Concrete Shells. 1994.
R 319. HANSEN, THOMAS CORNELIUS: Triaxial Tests with Concrete and Cement Paste. 1995.

Abonnement 1.7.1994 – 30.6.1995 kr. 130,–
Subscription rate 1.7.1994 – 30.6.1995 D.Kr. 130.–.

Hvis De ikke allerede modtager Afdelingens resuméoversigt ved udgivelsen, kan Afdelingen tilbyde at tilsende næste års resuméoversigt, når den udgives, dersom De udfylder og returnerer nedenstående kupon.

Returneres til
Afdelingen for Bærende Konstruktioner
Danmarks Tekniske Universitet
Bygning 118
2800 Lyngby

Fremtidig tilsendelse af resuméoversigter udbedes af
(bedes udfyldt med blokbogstaver):
Stilling og navn: .....
Adresse: .....
Postnr. og -distrikt: .....

The Department has pleasure in offering to send you a next year's list of summaries, free of charge. If you do not already receive it upon publication, kindly complete and return the coupon below.

To be returned to:
Department of Structural Engineering
Technical University of Denmark
Building 118
DK-2800 Lyngby, Denmark.

The undersigned wishes to receive the Department's List of Summaries:
(Please complete in block letters)
Title and name: .....
Address: .....
Postal No. and district: .....
Country: .....